Acoustic Power Control of a Lightly-Damped Enclosed Sound Field

Woo-Young Kim* and Dong-Kyu Kim**
Department of Aerospace Eng. Chosun University, Seosuk-dong 375, Gwangju City, Korea 501-759

Won-Gul Hwang***
Department of Mechanical Eng. Chonnam University, Yongbong-dong 300, Gwangju City, Korea 500-757

Abstract

This research attempts to find an active control strategy which reduces acoustic power and acoustic energy in lightly-damped enclosed sound field such as a vehicle compartment or an operating room of heavy industrial machinery. An active control strategy, which takes into consideration of the acoustic radiation power of the source as a cost function, is formulated and examined to find capability of reducing noise. An adaptive filtering algorithm for sound power control is suggested and implemented to control lightly-damped sound field.

To verify the method, sound power based active noise control algorithm was implemented on a rectangular box with lightly-damped wall, and popular acoustic energy based control with modal coupling reduction was performed to compare the noise reduction performance. It was shown that a total sound power based strategy provides a practical mean for global noise reduction for lightly damped sound field

Key Word : Acoustic power, Lightly damped enclosed sound filed, Adaptive algorithm

Introduction

Active noise control is based on two acoustic methods. The first is using destructive wave interference method, which can produce a quiet zone in a sound field through actuating a secondary source. The second is using a mutual coupling of sources to reduce the radiation efficiency of noise sources. It means that the secondary source tries to modify the characteristics of the sound source, while the first method reconstructs the sound field by superposition[1~3].

Since acoustic mode of an enclosed sound field is governed by standing wave and modal coupling, many researchers used an acoustic mode control method to reduce the acoustic pressure level. In this paper we compared two methods of active noise control strategies. The first was acoustic energy based control, and the second was acoustic power based control suggested in this paper. For an acoustic energy based control, we used a conventional Filtered - X LMS algorithm[4,5]. For the second control method, we developed a least mean product algorithm.

Sound power is an acoustic quantity which represents the capacity to generate sound[6~9]. The physical principle of radiation reduction is based on an acoustic coupling with another source

* Research Professor of Brain Korea 2
E-mail : inno@mail.chosun.ac.kr, TEL : 062-230-7274, FAX : 062-227-9942
** Professor
*** Professor

that confines a substantial portion of the acoustic volume flow into the near field of the sources. Since the active control for radiated sound power requires information only about the sound sources, it seems to be most effective to reduce total acoustic energy in an enclosed acoustic system.

We studied sound power based active noise control algorithm for a rectangular box with a lightly-damped wall. This method is compared with popular acoustic energy based control for noise reduction performance. We found that a total sound power based strategy provides a practical means for global noise reduction, and noise reduction performance depends on the acoustic coupling of sound sources and modal coupling.

Active noise control algorithm

Acoustic power control

An adaptive control strategy is generally used for active noise control. The most popular adaptation algorithm for acoustic energy control strategy is the least mean square algorithm such as Filtered-X LMS algorithm. Its characteristic is that reference input signal is compensated by transfer function of error path and speaker [4,5]. In acoustic energy based method, cost function can be described with 6 squared terms as equation(1). Since such a LMS formulation, in using DSP devices, causes computation time problem. Frequency range of control acoustic wave are depends on processing time, because D/A conversion sampling time should be required to generate smooth wave which can reduce acoustic mode amplitude in the control frequency range.

$$J=\frac{1}{2}E\left[q_p^2(t)+p_p^2(t)-\{q_p(t)-p_p(t)\}^2\right] + \frac{1}{2}E\left[q_s^2(t)+p_s^2(t)-\{q_s(t)-p_s(t)\}^2\right] \quad (1)$$

In this paper, we compared the conventional acoustic energy based control with acoustic power control for lightly-damped sound fields which includes a primary and a secondary source. We will suggest a practical adaptive control using acoustic power and test its performance. Now, we consider a single channel acoustic power control system in an enclosed sound field with a wall of acoustic impedance $Z(\omega)$, as shown in Fig. 1. The primary source strength $q_p(t)$ is assumed a stationary random process and $q_s(t)$ is coherent secondary source strength. Hereafter, subscripts p and q represent the primary and secondary sources respectively. The impulse response function if the system is expressed by an acoustic Green function $g_{ij}(t)$ in the time domain, which denotes acoustic pressure response at $\boldsymbol{r} = \boldsymbol{r}_i$ due to a source of a unit strength impulse at $\boldsymbol{r} = \boldsymbol{r}_j$.

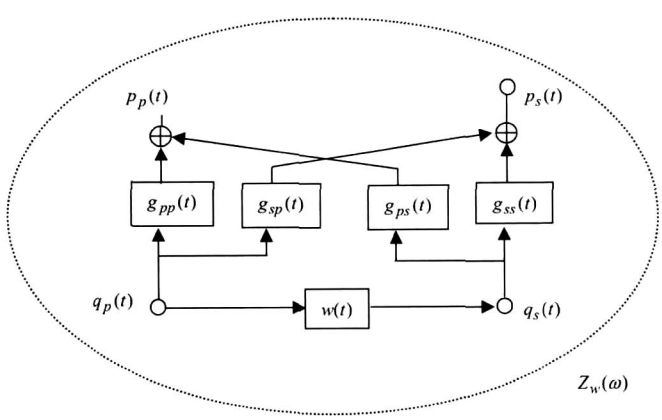

Fig. 1. Concept of active sound power control

We now wish to find the control filter $w(t)$ to minimize total acoustic power output of sources. We also want to estimate the maximum reduction of the acoustic potential energy in the enclosure for optimal filter. The filter output, that is, the secondary source strength can be expressed as follows;

$$q_s(t) = w(t) * q_p(t) \quad (2)$$

where * is a convolution operator. The acoustic pressure on the

primary and the secondary sources, $p_p(t)$and $p_s(t)$, can be written as equation (3),

$$\begin{aligned} p_p(t) &= g_{pp}(t) * q_p(t) + g_{ps}(t) * q_s(t) \\ p_s(t) &= g_{sp}(t) * q_p(t) + g_{ss}(t) * q_s(t) \end{aligned} \tag{3}$$

Adaptive filtering for single channel acoustic power control

We now consider the adaptive implementations of FIR (finite impulse response) digital filter to minimize the total sound power in the single channel control system. Basically, the acoustic power control algorithm is derived using finite cost function and steepest descent strategy. The cost function to be minimized is the total acoustic power of the sources. Assuming a stationary random processes, the averaged total acoustic power due to the primary and secondary source can be expressed as

$$J = E[\, q_p(t) p_p(t) + q_s(t) p_s(t)] \tag{4}$$

where $E[\,\cdot\,]$ denotes the ensemble average operator.

The adaptive digital filter of length M at step k can be expressed as follows;

$$\boldsymbol{w_k} = [\, w_k(0) \;\; w_k(1) \;\cdots\; w_k(M-1)]^T \tag{5}$$

We suggest the least mean product adaptive algorithm using steepest descent method to reduce calculation time for updating $\boldsymbol{w_k}$. According to the steepest descent method, the adaptive filter update equation is given as

$$\boldsymbol{w_{k+1}} = \boldsymbol{w_k} - \mu \frac{\partial \hat{J}}{\partial \boldsymbol{w_k}} \tag{6}$$

where μ is a positive convergence constant.

To derive the adaptive algorithm, let us approximate the control function, which is a time averaged total sound power as follows;

$$\hat{J}(k) = \sum_{i=k}^{k-M+1} \{ q_p(i) p_p(i) + q_s(i) p_s(i) \} \tag{7}$$

where M is a number of steps of averaging the instantaneous total sound power $\hat{J}$ at step k, $q_p(i)$, $p_p(i)$, $q_s(i)$ and $p_s(i)$ are discrete time histories of $q_p(t)$, $p_p(t)$, $q_s(t)$ and $p_s(t)$, and i is discrete time. According to the equation(2) we can get relationships which are expressed by equation(8)

$$\begin{aligned} p_p(k) &= H_{pp}^T \boldsymbol{q_p}(k) + H_{ps}^T \boldsymbol{q_s}(k) \\ p_s(k) &= H_{sp}^T \boldsymbol{q_p}(k) + H_{ss}^T \boldsymbol{q_s}(k) \end{aligned} \tag{8}$$

where volume velocity vectors of the primary and secondary sources at step k are defined as $\boldsymbol{q_p}(k)$ and $\boldsymbol{q_s}(k)$, and acoustic pressure vectors of the primary and secondary sources at step k are defined as $\boldsymbol{p_p}(k)$ and $\boldsymbol{p_s}(k)$ as follows;

$$\begin{aligned} \boldsymbol{q_p}(k) &= [\, q_p(k), q_p(k-1), \cdots, q_p(k-M+1)]^T \\ \boldsymbol{q_s}(k) &= [\, q_s(k), q_s(k-1), \cdots, q_s(k-M+1)]^T \\ \boldsymbol{p_p}(k) &= [\, p_p(k), p_p(k-1), \cdots, p_p(k-M+1)]^T \\ \boldsymbol{p_s}(k) &= [\, p_s(k), p_s(k-1), \cdots, p_s(k-M+1)]^T \end{aligned} \tag{9}$$

Similarly, we introduced H_{ij} as follows;

$$H_{ij} = [\, g_{ij}(0) g_{ij}(1) \cdots g_{ij}(M-1)]^T \tag{10}$$

where $g_{ij}(k)$ is impulse response of Green function $G_{ij}(\,\cdot\,)$. Substituting equations(8)~(10) to equation(7), Since $\boldsymbol{q_p}$ is not related to the weighting vector $\boldsymbol{w_k}$, using relationship given by equation(3), we obtain

$$\frac{\partial \hat{J}}{\partial \boldsymbol{w}_k} = \sum_{i=k}^{k-M+1}\left[\frac{\partial q_p(i)}{\partial \boldsymbol{w}_k} p_p(i) + q_p(i)\frac{\partial p_p(i)}{\partial \boldsymbol{w}_k} + q_s(i)\frac{\partial p_s(i)}{\partial \boldsymbol{w}_k}\right]$$

$$= \sum_{i=k}^{k-M+1}\left[q_p(i)\frac{\partial\{H_{pp}^T \boldsymbol{q}_p(i) + H_{ps}^T \boldsymbol{q}_s(i)\}}{\partial \boldsymbol{w}_k} + \frac{\partial \boldsymbol{w}_k^T \boldsymbol{q}_p(i)}{\partial \boldsymbol{w}_k} p_s(i) + q_p(i)\frac{\partial\{H_{sp}^T \boldsymbol{q}_p(i) + H_{ss}^T \boldsymbol{q}_s(i)\}}{\partial \boldsymbol{w}_k}\right]$$

$$= \sum_{i=k}^{k-M+1}\left[q_p(i)\frac{\partial\{H_{pp}^T \boldsymbol{q}_p(i) + H_{ps}^T \boldsymbol{w}_k^T \boldsymbol{Q}_p(i)\}}{\partial \boldsymbol{w}_k} + \frac{\partial \boldsymbol{w}_k^T \boldsymbol{q}_p(i)}{\partial \boldsymbol{w}_k} p_s(i) + q_s(i)\frac{\partial\{H_{sp}^T \boldsymbol{q}_p(i) + H_{ss}^T \boldsymbol{w}_k^T \boldsymbol{Q}_p(i)\}}{\partial \boldsymbol{w}_k}\right] \tag{11}$$

where $\boldsymbol{Q}_p(i)$ is a symmetrical matrix which is constructed as follow;

$$\boldsymbol{Q}_p(i) = [\boldsymbol{q}_p(i), \boldsymbol{q}_p(i-1), \cdots, \boldsymbol{q}_p(i-M+1)]^T. \tag{12}$$

Equation(11) can be modified as

$$\frac{\partial \hat{J}}{\partial \boldsymbol{w}_k} = \sum_{i=k}^{k-M+1}\left[q_{p(i)}\frac{\partial H_{ps}^T\{\boldsymbol{w}_k^T \boldsymbol{Q}_p(i)\}}{\partial \boldsymbol{w}_k} + \boldsymbol{q}_p^T(i) p_s(i) + q_s(i)\frac{\partial H_{ss}^T\{\boldsymbol{w}_k^T \boldsymbol{Q}_p(i)\}}{\partial \boldsymbol{w}_k}\right]$$

$$= \sum_{i=k}^{k-M+1}\left[q_p(i)\{H_{ps}^T \boldsymbol{Q}_p(i)\} + \boldsymbol{q}_p^T(i) p_s(i) + q_s(i)\{H_{ss}^T \boldsymbol{Q}_p(i)\}\right]. \tag{13}$$

Substituting equation(13) to equation(7), we obtain update equation as

$$\boldsymbol{w}_{k+1} = \boldsymbol{w}_k - \mu \sum_{i=k}^{k-M+1}\left[q_p(i)\{H_{ps}^T \boldsymbol{Q}_p(i)\} + \boldsymbol{q}_p^T(i) p_s(i) + q_s(i)\{H_{ss}^T \boldsymbol{Q}_p(i)\}\right]. \tag{14}$$

This adaptation algorithm includes product terms of acoustic pressure and volume velocity. We found that the least mean square form of the acoustic power control algorithm has only 3 terms, but if we use least square from, 6 mean squared terms of error[12]. We implemented real time acoustic power control using a block diagram which has a least mean product form adaptation algorithm as shown in Fig.2.

There is a difference in using the reference signal between the acoustic energy control and acoustic power control. In acoustic power control, the volume velocity signal of a primary source is used as reference input. Because of such a difference, we need to measure the volume velocity signal of the primary and secondary sources. We used an intensity probe which has closely spaced 2 microphones to measure the acoustic power. Sound power was estimated using product of acoustic intensity vector and sound radiation area of a speaker which is used as an acoustic source.

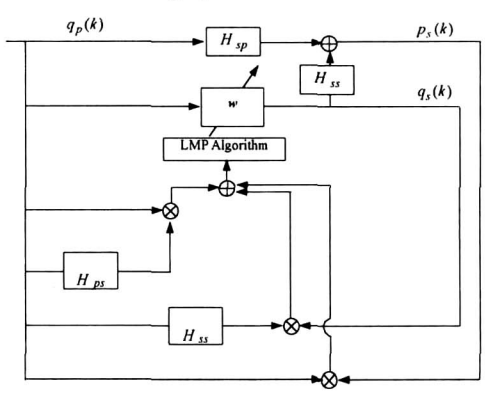

Fig. 2. Block diagram of least mean product adaptive algorithm

Experiments and Discussions

Experimental Setup

We constructed a rectangular acoustic field with a primary and a secondary sources. Impedance of wall surface is constant, $Z_s(\boldsymbol{r}_s)/\rho c = 0.2 + j3.0$, dimension of a sound field is $L_x \times L_y \times L_z = 1.3m \times 1.7m \times 1.0m$. Acoustic impedance $Z(\boldsymbol{r}_s)$ is such that $|Z(\boldsymbol{r}_s)| \gg 1$, so that it can be assumed the wall surface is sufficiently rigid.

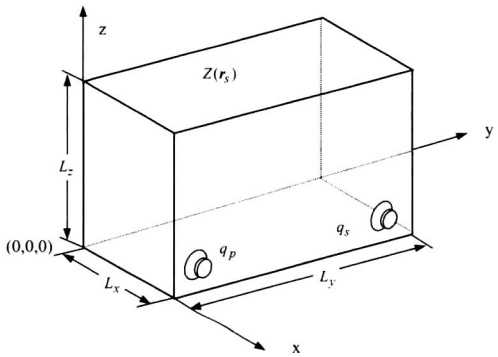

Fig. 3. Simulation and experiment model for three dimensional rectangular enclosure with a primary source of strength q_p and a secondary one of strength q_s

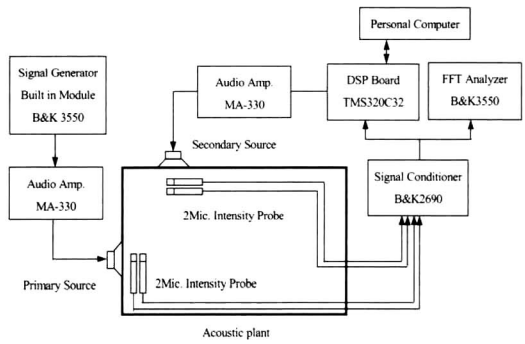

Fig. 4. Experimental setup using 2-intensity probes

A lightly-damped sound field was made with acrylic-plates. Full range single-cone speakers are used for both primary and secondary sources, and its available low frequency is 80Hz. Fig. 4 shows the block diagram of the experimental setup for acoustic power control. To measure acoustic pressure, we used microphones of sensitivities of 50mV/Pa. A 4 channel FFT analyzer was used for data acquisition and analysis. The filter order 100 was selected to identify acoustic plants and the weighting vector for controller.

Results and discussion

We know that noise reduction level can be determined by insertion loss according to the change of the secondary source location. So we chose two locations of the secondary source based on the insertion loss calculated using a equation of acoustic coupling [12]. We performed the experiment at the two positions of secondary source. As shown in Table 3.1, the location ① has the same direction with the primary source, and location ② has a perpendicular direction with the primary source. In the first experiment, acoustic energy is chosen as a cost function, and in the second acoustic power is chosen. Acoustic pressure reduction performance is compared to evaluate two control strategies which are Filtreed-X LMS algorithm[4,5] using acoustic pressure signal of error microphone and acoustic power control LMP algorithm. We used 3 types of excitation signals; sinusoidal signal, band-passed white noise with a central band frequency of 150 Hz, and band pass frequency range of 100Hz, and a low-passed white noise with a cut-off frequency of 400Hz.

Table 1. Available source positions

Secondary source	x[m]	y[m]	z[m]
position ①	1.3	1.535	0.165
position ②	1.135	0.0	0.165

Sinusoidal excitation

To evaluate the attenuation performance, we used sinusoidal signals whose frequency consist with acoustic modal frequencies of enclosure. Fig. 5 shows the results of acoustic pressure history at the error microphone for a 100Hz sinusoidal excitation. When the secondary source is located at position ①, noise reduction of 32dB was obtained by acoustic energy control, and 28dB by acoustic power control. For the position ②, noise reduction of 30dB was

obtained by acoustic energy control, and 32.8dB by acoustic power control. These results show that there was an equal level of noise reduction for either method.

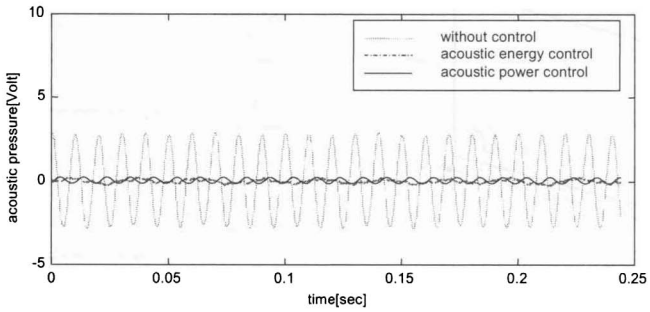

Fig. 5. Comparison of acoustic pressure signal of the error microphone (secondary source position ①)

Narrow band-passed white noise excitation

To evaluate the attenuation performance for low frequency range excitation which includes dominant components of acoustic modes, we used narrow band-passed white noise. The central frequency of excitation signal was 150Hz, and the band-pass range was 100Hz. Fig. 6 and Fig. 7 illustrate the results of each acoustic pressure signal for narrow band-passed white noise excitation. From the auto spectrum of acoustic pressure, better noise reduction is achieved with the secondary source at position ② than at position ①.. Table 2 shows the comparison results of peak values of acoustic pressure signals, and table 3 shows the results of RMS values which was calculated using the error microphone signal. From these results, we can achieve a better noise reduction when the secondary source is located at position ②.

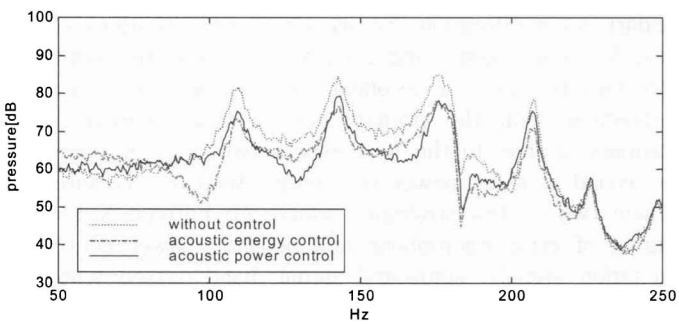

Fig. 6. Comparison of acoustic pressure spectrum at the error microphone (secondary source position ①)

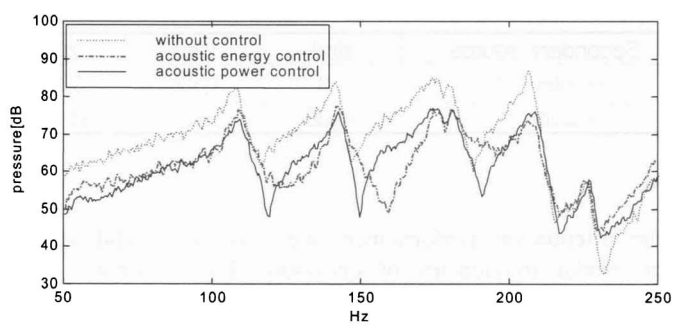

Fig. 7. Comparison of acoustic pressure spectrum at the error microphone (secondary source position ②)

Table 2. Comparison of acoustic pressure level of error microphone (unit : dB)

mode	Secondary source position ①			Secondary source position ②		
	without control	energy control	power control	without control	energy control	power control
I	80.7	76.5	77.1	81.9	75.6	73.1
II	82.6	80.1	81.5	83.1	77.4	76.8
III	82.9	81.6	80.1	83.8	76.7	77.1
IV	77.4	72.9	76.7	83.8	72.6	76.5

Table 3. Comparison of the RMS value of pressure histories of the error microphone

Secondary source position	without control	acoustic energy control	acoustic power control
①	0.276	0.221	0.240
②	0.418	0.237	0.229

Low-passed white noise excitation

To evaluate attenuation performance of overall frequency range which is supposed to be under the real time control, we used low-passed white noise signal which has a cut-off frequency of 400Hz. Fig. 8 and Fig. 9 illustrate the comparison results for acoustic pressure spectrum at the error microphone. Table 4 shows the comparison results of the peak values at 5 dominant modes. These experimental results show similar trend as band-passed white noise excitation, so we achieved a better noise reduction when the secondary source is located at position ② than at position ①.

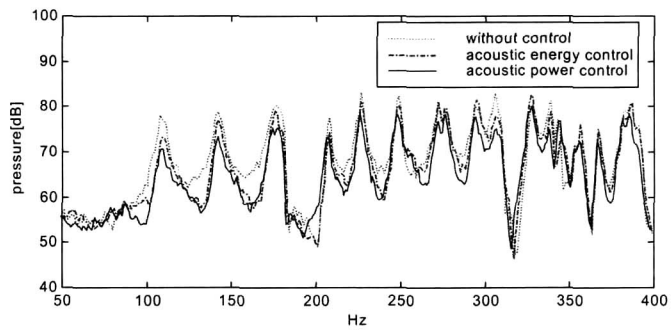

Fig. 8. Comparison of acoustic pressure magnitude spectrum of the error microphone (secondary source position ①)

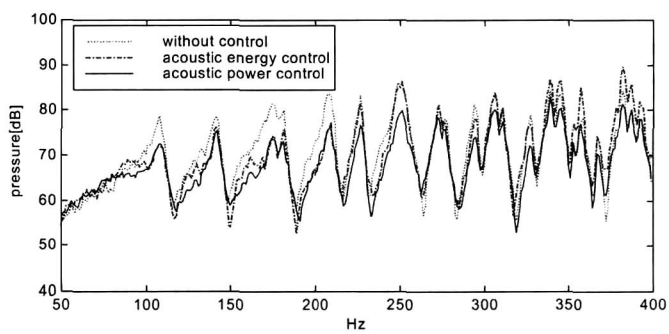

Fig. 9. Comparison of acoustic pressure magnitude spectrum of the error microphone (secondary source position ②)

Table 4. Comparison of acoustic pressure level of error microphone (unit : dB)

mode	Secondary source position ①			Secondary source position ②		
	without control	energy control	power control	without control	energy control	power control
I	77.8	72.3	72.6	78.5	71.8	71.6
II	78.7	77.1	75.6	78.6	76.8	76.1
III	80.1	79.3	77.7	81.3	77.4	76.2
IV	77.5	73.3	75.5	82.4	79.9	77.3
V	82.8	81.1	81.1	82.2	80.9	80.6

Conclusions

We introduced acoustic power control concept to reduce noise for lightly-damped sound field, and suggested a least mean adaptive algorithm for real time acoustic power control, as shown below:

$$\boldsymbol{w}_{k+1} = \boldsymbol{w}_k - \mu \sum_{i=k}^{k-M+1} \left[q_p(i) \{ H_{ps}^T \boldsymbol{Q}_p(i) \} + \boldsymbol{q}_p^T(i) p_s(i) + q_s(i) \{ H_{ss}^T \boldsymbol{Q}_p(i) \} \right]$$

This algorithm has only 3 product terms, which means we can save calculation time and memory. We implemented a real-time active acoustic power control for a rectangular-shaped structure with an acoustically rigid wall.

We found a better performance when the secondary source is located at the strongly acoustically coupled position. Thus, we need to consider coupling effect of the acoustic mode and the acoustic source. In the case where the position of the control source is the same, we found an same level of noise reduction with conventional acoustic energy based control by using a acoustic power control strategy. We estimated such a characteristic caused by two reasons, one is enclosed sound field consists of walls with uniform acoustic impedance, and the other is the boundary has a geometrically simple shape like a rectangular box.

For the future work, we need to find strategy for multi-channel control, which we can effectively enlarge the zone of quiet. To implement general case such as interior of vehicle which has geometrically complex shape and non-uniform acoustic properties, we also have to try to develop an effective techniques of signal processing and a control algorithm using reverberation time or a wall reflection coefficient of lightly-damped enclosed sound fields.

References

[1] C. Bao, P. Sas, and H. Brussel, 1992," Adaptive Active Control of Noise in 3-D Reverberant Enclosure, "*J. of Sound and Vibration*, Vol. 161(3), pp. 501-514, 1992.

[2] A.J. Vullmore, P.A. Nelson, A.R.D. Curtis, and S.J. Elliott, 1987," The Active Minimization of Harmonic Enclosed Sound Fields, Part I : A Computer Simulation, *J. of Sound and Vibration*, Vol. 117(1), pp. 15-33.

[3] S.J. Elliott, A.R.D. Curtis, A.J.Vullmore, and P.A. Nelson, 1987, "The Active Minimization of Harmonic Enclosed Sound Fields, Part II : Experimental Verification, " *J. of Sound and Vibration*, Vol. 117(1), pp. 35~58.

[4] S.J. Elliott, and P.A. Nelson, 1985, "Algorithm for Multi-channel LMS Adaptation Filtering, ,"*Electronic Letters* , Vol. 21, pp. 979~981.

[5] L.J. Eriksson, 1991, "Development of Filtered-U Algorithm for Active Noise

Control, "*J. of Acoust. Soc. Am.*, Vol. 89(1) , pp. 257~265.

[6] F.T. Agerkvist, and F. Jacobsen, 1992, "Sound Power Determination in Reverberation Rooms at Low Frequencies, "*J. of Sound and Vibration*, Vol. 166(1), pp. 179~190.

[7] U.S. Shirabatti, and M.J. Crocker, 1992, "Studies on Sound Power Measurements Using the Sound Intensity Technique, "*Noise Control Engineering Journal*, Vol. 41, No. 2, pp. 323~330.

[8] F.J. Fahy, 1997, "International Standards for the Determination of Sound Power Levels of Sources Using Sound Intensity Measurement : an Exposition, "*Applied Acoustics*, Vol. 50, no. 2, pp. 97~109.

[9] U.S. Shirahatti, and M.J. Crocker, 1993, "Studies on the Sound Power Estimation of a Noise Source Using the Two-Microphone Sound Intensity Technique, "*Acoustica*, Vol. 80, pp. 378~396.

[10] P.A. Nelson, A.R.D. Curtis, S.J. Elliott, and A.J. Bullmore, 1987 "The Minimum Power Output of Free Field Point Sources and Active Noise Control, "*J. of Sound and Vibration*, Vol. 116, pp. 397~414.

[11] W.Y. Kim, 1999, *Active Noise Control of 3-Dimensional Lightly Damped Enclosed Sound Field*, Ph.D.Thesis, Chonnam National University.

[12] S.W. Kang, and Y.H. Kim, 1997, "Causally Constrained Active Sound Power Control in an Enclosed Space, "*J. of Sound Vibration*, Vol. 204(5), pp. 807~822.